This full text paper was peer reviewed at the direction of IEEE Communications Society subject matter experts for publication in the ICC 2007 proceedings.

Multipath-Resistant Incoherent Space-Time Codes for IR-UWB MIMO Systems

Enzo Baccarelli, Mauro Biagi, Cristian Pelizzoni, Nicola Cordeschi
{enzobac, biagi, pelcris, cordeschi }@infocom.uniroma1.it

***Abstract*— In this contribution we develop a Multiple-Input Multiple-Output (MIMO) Impulse Radio Ultra Wide Band (IR-UWB) transceiver for Orthogonal signalling over (baseband) *multipath* faded MIMO channels. The proposed Maximum-Likelihood receiver results to be "partially coherent", since it is optimized to work without any information about channel coefficients, and it is based on the knowledge of the arrivals' times of the transmitted signals' replicas. The behavior of the proposed transceiver has been evaluated via three suitable versions of the Union-Chernoff Bound related to several indoor and outdoor propagation scenarios, and these limits are considered to introduce a novel family of unitary orthogonal Space-time Block Codes (e.g., the Space-Time OPPM (STOPPM) codes), that are able *to attain* maximum diversity and coding gains.**

***Keywords*— IR-UWB, multipath faded MIMO channels, Space-Time Block Codes (STBCs), STOPPM codes.**

I. Motivation and main contributions

In the recent years, "everywhere" connectivity is assuming a key-role for the implementation of the Wireless Networks. In order to achieve this target, several new solutions are arising to link nomadic users to Internet via Broadband Wireless Access (BWA) [16]. Up to now, one of the most promising wireless technology seems to be the IR-UWB one, currently considered in the framework of the IEEE 802.15.4 group for Wireless Personal Area Network (WPAN). Since IR-UWB systems have to follow the emission constrains imposed by FCC [7], [8, Chap.10], they radiate much less power than IEEE 802.11-like systems [8, Appendix 10.c], [14], so that their coverage ranges are limited up to few meters. Specifically, the IR-UWB physical layer for the IEEE 802.15.3a should provide net data rate of 110 Mbps at 20 mt, or higher at shorter distances [8, Chap. 10], [14]. Hence, in order to be proposed as a possible competitor of WLAN technologies, in the emerging segment of BWA applications, the current coverage ranges of IR-UWB systems should be increased of (at least) one order of magnitude. Since a key-capability of multi-antenna is to improve coverage range and conveyed throughput *without increasing* the radiated power and loosing in performance [11], in principle the IR-UWB and multi-antenna paradigm could be merged into a suitable MIMO IR-UWB system to meet the coverage requirements of 4G-WLANs.

Enzo Baccarelli, Mauro Biagi, Cristian Pelizzoni and Nicola Cordeschi are with INFO-COM Dept., University of Rome "La Sapienza", via Eudossiana 18, 00184 Rome, Italy. Ph. no. +39 06 44585466 FAX no. +39 06 4873330.
This work has been partially supported by the Italian National project: "Wireless 8O2.16 Multi-antenna mEsh Networks (WOMEN)" under grant number 2005093248.

A. Previous related works

Up till now, IR-UWB transceiver design has been mainly limited to single-antenna architectures for short-range communications ([1,10],[8, Chaps. 5, 6 and references therein]). Overall, several SISO IR-UWB transceivers employing Rake-receiver have been proposed and mainly tested under the (optimistic) assumption of perfect channel knowledge. Furthermore, they do not properly exploit the multipath effect of the IR-UWB channel in order to increase the system diversity (see, for example, Chap.6 of [8] for an overview on this topic). About MIMO IR-UWB systems, an analog version of the Alamouti code has been presented in [2,4] for the case of IR-UWB systems, equipped with two-transmit and one-received antennas. Lastly, in [21] a MIMO IR-UWB system with *uncoded* 2-PAM modulation format is employed, while the receiver is composed by a zero forcing block followed by Rake receiver. In the above mentioned work, the energy is *not* considered as scattered over "Multiple Poisson distributed paths Clusters" as reported in [18], but they are assumed to be equally and temporally spaced.

II. System model

A. Transmitted signal

Let us consider now a point-to-point UWB link, composed by N_t transmit and N_r receive antennas. The source generates an L-ary ($L \geq 2$) information symbol $b \in \{0, 1, ..., L-1\}$ at each signalling period T_s(sec.) mapped into N_t OPPM M-ary baseband analog signals assuming the usual expression for UWB systems [1,2,4,15] as in

$$x^{(i)}(t) \triangleq \sum_{m=0}^{N_f-1} \sqrt{\frac{E_f}{N_t}} p(t - mT_f - d_i T_p), 0 \leq i \leq N_t \ \ , 0 \leq t \leq T_s, \tag{1}$$

where $d_i \in \{0, ..., M-1\}$ stands for the M-ary ($M \geq 2$) PPM symbol emitted by the i-th transmit antenna. The stream of N_t PPM symbols is adopted for Space-Time (ST) coding of the information L-ary symbols. The unit energy UWB baseband pulse $p(t)$ presents time duration T_p(sec.) and it is repeated N_f times over each T_s. As a consequence, the signalling period is divided into N_f frame periods T_f(sec.) (e.g., $T_s = N_f T_f$) and in order to avoid severe Inter-Pulse Interference (IPI), this last has been set as $T_f = MT_p + T_\mu$, where T_μ(sec.) denotes the multipath delay spread typically experienced by UWB channels. Finally, E_f (Joule) denotes the energy globally spent by the N_t transmit antennas over each T_f.

1-4244-0353-7/07/$25.00 ©2007 IEEE

B. Received Signal

The UWB systems are affected by highly frequency selective fading, and the energy of the received signals is scattered over a number of resolvable multipath components. Specifically, according to [17], the statistical MIMO UWB-IR channel model is described by $(N_t \times N_r)$ SISO time dispersive channel responses as

$$h_{ji}(t) \triangleq \sum_{q=0}^{Q-1} \sum_{n=0}^{V-1} h_{q,n}(j,i)\delta\left(t - T_q - \tau_{q,n}\right), \qquad (2)$$
$$1 \le i \le N_t,\ 1 \le j \le N_r,$$

where $\delta(t)$ stands for the Dirac delta function. According to the "Multiple Cluster Poisson channel Model" [18], each SISO response is composed by different clusters, accounted by the q index sum in (2) and arriving at the T_q time. The q-th cluster is constituted by a number of arrivals, delayed of $\tau_{q,n}$ and accounted in (2) by the n sum index. Both numbers of clusters and corresponding arrivals are Poisson distributed with mean frequencies Λns^{-1} and λns^{-1}. The fading coefficient $h_{q,n}(j,i)$ from the i-th transmit antenna to j-th receive one, referred to n-th arrival of the q-th cluster, can be modeled as (see [18]) $h_n(j,i) = \beta_n(j,i)\alpha_n(j,i)$, where $\alpha_n(j,i)$ is the magnitude term and $\beta_n(j,i) \in \{-1,1\}$ stands for the (i.i.d.) random-phase due to possible reflections. We have considered three different magnitude distributions according to the current literature when different propagation scenarios ranging from indoor NLOS to outdoor LOS environments [8]. Furthermore, the fading coefficients are assumed spatially uncorrelated. According to [18], we consider the channel Multiple Intense Profile (MIP) as double exponentially decreasing so that $\mathrm{E}\left\{\mid h_n(j,i) \mid^2\right\} = \Omega_0 e^{-T_q/\Gamma} e^{-\tau_{n,q}/\gamma}$, where $\mathrm{E}\{.\}$ denotes expectation, and $\left(\Omega_0 \triangleq \sum_{q=0}^{Q-1}\sum_{n=0}^{V-1} e^{-\tau_{q,n}/\gamma}\right)$ is set to normalize the energy contained in all the $(V \times Q)$ paths. Now, due to their nature, UWB channels experience double exponentially decreasing MIPs and most of the channel models are characterized by the cluster mean frequency one order higher than the arrivals' one (e.g., $\Lambda \gg \lambda$). Thus, only the arrivals within the first cluster (also according to [8]) have to be detected, while the rest of them can be neglected. Hence, we reduce the "Multiple Cluster Poisson Channel Model" to the "Single Poisson Channel Model", by only considering the arrivals with $q = 0$, and for sake of simplicity we replace the notation $\{\tau_{0,0}, ..., \tau_{0,V}\}$ with $\{\tau_0, ..., \tau_V\}$ and $\{h_{0,n}(j,i)\}$ with $\{h_n(j,i)\}$. We consider the receive signal $y_j(t)$ at the j-th receive antenna is expressed as

$$y_j(t) = \sum_{i=1}^{N_t} x^{(i)}(t) \circledast h_{ji}(t)$$
$$= \sum_{i=1}^{N_t}\sum_{n=0}^{V-1} h_n(j,i)x^{(i)}(t-\tau_n) + w_j(t),\ \ 1 \le j \le N_r, \quad (3)$$

where $w_j(t)$ is a real zero-mean white Gaussian noise with a two side power spectral density $\mathcal{N}_0/2$, while the operator $\circledast$ stands for analog convolution. The number of paths is limited by the ratio T_μ/T_p with $T_\mu = 30$ns and $T_p = 0.7$ns.

C. "Orthogonality Property" for transmit pulses

An accurate setting for T_p is finalized to avoid overlapping of different M-OPPM symbols at the receive side, so to be still orthogonal as in

$$\int_{-\infty}^{+\infty} p(t - mT_p - \tau_f)p(t - lT_p - \tau_q)dt \triangleq$$
$$\rho((l-m)T_p + (\tau_f - \tau_q)) \begin{cases} 1, & \text{for l=m and f=q,} \\ 0, & \text{otherwise,} \end{cases} \qquad (4)$$

where $\rho(.)$ denotes the autocorrelation of $p(t)$. If the "Orthogonality property" expressed in (4) is not satisfied, then the overall system results to be affected by spatial Inter Pulse Interference (IPI) which, as detailed in Sect.VI.C, *significantly reduces* the corresponding performance specially for highly scattered and time dispersive channels (e.g., CM3). From (4) we may note that the inter-arrivals $\{\Delta_i\}$ are required to be temporally-spaced (at least) of MT_p(sec.). Therefore, by considering that the inter-arrivals are exponentially distributed we conclude that the Orthogonality property is retained for the $(1-\eta)\%$ of the service time, e.g., $P\{\Delta_i \ge MT_p\} \le 10^{-2}$, only if the pulse width is upper limited as follows:

$$T_p \le -\frac{\ln(1-\eta)}{\lambda M}. \qquad (5)$$

III. Space-Time codes over M-ary OPPM modulation

The ultimate task of the receiver is to compute the ML decision $\hat{b}_{ML}$ on the currently transmitted information symbol b, by exploiting the received signals $\{y_j(t),\ 1 \le j \le N_r\}$ in (3) and the information on the arrivals times $\{\tau_n,\ 0 \le n \le V\}$. Let us consider now an equivalent matrix representation for the (analog) MIMO IR-UWB channel in (2). In this regard, it is important to consider that the output of matched filters the to M-ary OPPM pulses and their overall replicas are expressed as follows

$$y_j(l,n) \triangleq \frac{1}{\sqrt{N_f}} \int_0^{T_s} y_j(t) \left[\sum_{k=0}^{N_f-1} p(t - kT_f - lT_p - \tau_n)\right] dt,$$
$$0 \le l \le M-1, 1 \le j \le N_r,\ 0 \le n \le V. \quad (6)$$

These scalar terms constitute a set of $(M \times N_r(V+1))$ statistics resulting to be *sufficient* for the ML detection of the transmitted information symbol [5,17]. Thus, after replacing $y_j(t)$ in (6) by definition reported in (3), and by exploiting the "Orthogonality property" in (4), we can rewrite (6) as

$$y_j(l,n) = \sqrt{\frac{\gamma_b N_f \lg_2 L}{N_t}} \sum_{i=1}^{N_t} h_n(j,i)\phi_i(l) + w_j(l,n)$$
$$1 \le j \le N_r,\ 0 \le n \le V. \qquad (7)$$

where

$$\phi_i(l) \triangleq \frac{1}{N_f} \int_0^{T_s} p(t - kT_s - d_iT_p - \tau_n)p(t - kT_s - lT_p - \tau_n)dt$$

$$\equiv \begin{cases} 1, \text{ for } d_i = l \\ 0, \text{ otherwise,} \end{cases} \quad (8)$$

and the noise terms

$$w_j(l,n) \triangleq \frac{1}{\sqrt{N_f}} \sum_{k=0}^{N_f-1} \int_0^{T_s} w_j(t) p(t - kT_s - \tau_n) dt,$$

$$0 \le l \le M-1,\ 0 \le l \le M-1,\ 1 \le j \le N_r,\ 0 \le n \le V, \quad (9)$$

in (7) are real-valued, zero mean, mutually uncorrelated unit-variance Gaussian ($\mathcal{G}$) r.v.s. Therefore, after indicating as $\mathbf{Y} \triangleq [\mathbf{Y}_1 \ ... \ \mathbf{Y}_{N_r}]$ the $(M \times N_r(V+1))$ blocks matrix constituted by $(M \times (V+1))$ matrices $\{\mathbf{Y}_j,\ 1 \le j \le N_r\}$ that are employed to collect the terms[1] $y_j(l,n)$ in (7), we may recast the relationship in (7) in the following form

$$\mathbf{Y} = \sqrt{\frac{\gamma_b N_f \lg_2 L}{N_t}} \mathbf{\Phi H} + \mathbf{W}, \quad (10)$$

where $\mathbf{W}$ denotes the $(M \times N_r(V+1))$ matrix collecting the noise terms in (9), $\mathbf{H}$ stands for the $(N_t \times N_r(V+1))$ matrix of the MIMO channel coefficients $\{h_n(j,i)\}$, while $\mathbf{\Phi}$ is the $(M \times N_t)$ matrix composed by the binary-valued coefficients in (8). Specifically, $\mathbf{\Phi}$ in (10) represents the space-time matrix codeword associated to the (ordered) N_t-ple $\{d_1, .., d_{N_t}\}$ of M-ary OPPM data radiated by the transmit antenna (see (1)). About the generic codeword of $\mathbf{\Phi}$, directly from (8) it follows that, when $d_i = l,\ \in \{0, ..., (M-1)\}$, thus the i-th codeword $\mathbf{\Phi}$ is binary and its columns are constrained to be unit-vectors of $\mathbb{R}^M$.

A. Some Key-properties of the OPPM-based Space-Time Block Codes

Since the multi-antenna transmitter maps each l value assumed by the information symbol b into a corresponding (matrix) value $\mathbf{\Phi}_l$, assumed by the transmitted space-time codeword $\mathbf{\Phi}$, thus, from a statistical point of view, $\mathbf{\Phi}$ in (10) is an L-ary r.v. whose outcomes $\left\{\mathbf{\Phi}_l \in \{0,1\}^M \times \{0,1\}^{N_t},\ 0 \le l \le L-1\right\}$ are equiprobable and constitute the codewords of the resulting Space-Time Block Code (STBC). Specifically, the l-th codeword $\mathbf{\Phi}_l$ is biunivocally associated to the l-th information symbol $b = l$ (e.g., $\mathbf{\Phi}_l \rightleftarrows b = l$). Furthermore, the relationship (8) dictates the following structure for $\mathbf{\Phi}_l$:

$$\mathbf{\Phi}_l = [\underline{\mathbf{e}}_1^{(l)} ... \underline{\mathbf{e}}_{N_t}^{(l)}] \leftrightarrow\ b = l,\ \ 0 \le l \le L-1, \quad (11)$$

where the ordered sequence of N_t unit-vectors of $\mathbb{R}^M$, constituting the columns of $\mathbf{\Phi}_l$, depends on the value l actually assumed by the transmitted information symbol b.

[1]The scalar term $y_j(l,n)$ in (7) constitutes the $((l+1) \times (n+1))$-th entry of the matrix $\mathbf{Y}_j$, composing the block j of the matrix $\mathbf{Y}$ defined in (10). Similarly, $h_j(i,n)$ and $w_j(l,n)$ denote the $(i \times (n+1))$-th and $((l+1) \times (n+1))$-th entries of the blocks $\mathbf{H}_j$ and $\mathbf{W}_j$ of $\mathbf{H}$ and $\mathbf{W}$, respectively.

IV. ML Decoding of OPPM-based Unitary STBCs and Related Performance

Since the results in the above sections pointed out that received sequences in (10) results to be sufficient statistic for the ML detection on the transmitted symbol b, and, in addition, each information symbol $b = l$ is biunivocally associated to the corresponding (matrix) codeword $\mathbf{\Phi}_l$ (see eq.11), thus the decision rule implemented by the ML detector may be directly posed in the following form:

$$\hat{\mathbf{\Phi}}_{ML} = \underset{0 \le l \le L-1}{\arg\max} \left\{ p\left(\mathbf{Y} \mid \mathbf{\Phi}_l, \right) \right\}, \quad (12)$$

where $p(. \mid .)$ in (12) is the pdf of $\mathbf{Y}$ conditioned on $\mathbf{\Phi}_l$. Now, several results (reported for example in [6, 12, 13] and references therein) lead to the conclusion that Unitary STBCs may approach to the Shannon capacity of MIMO faded links, so that, these codes appears to be appealing ([5, 11, 14] and reference therein). Thus, since also the STOPPM codes we have introduced in Sect.III are unitary, in the sequel we focus on unitary STBCs. Specifically, for Unitary STBCs, the ML decision rule (12) assumes the following form:

$$\hat{\mathbf{\Phi}}_{ML} = \underset{0 \le l \le L-1}{\arg\max} \{z_l\} \quad (13)$$

where z_l is differently defined for Gaussian ($\mathcal{G}$), Nakagami ($\mathcal{N}K$) and Log-Normal ($Lg\mathcal{N}$) path gains pdfs. Specifically, for ($\mathcal{G}$) pdf

$$z_l \triangleq \sum_{n=0}^{V+1} \sum_{j=1}^{N_r} \sum_{i=1}^{N_t} \chi_n (\underline{\mathbf{y}}_j(n)^T \underline{\mathbf{e}}_i(l))^2,\ \ l = 0, ..., L-1, \quad (14.1)$$

where

$$\chi_n \triangleq \left(1 + \frac{1}{\gamma_b} \frac{N_t}{\sigma_h^2(n) N_f \lg_2 L}\right)^{-1},\ \ 0 \le n \le V. \quad (14.2)$$

Let us note that the term in (14.2) acts as weighting coefficient of the corresponding path gains coming at the n-th arrival time, and specifically it reduces to

$$\chi_n = \begin{cases} 0, \text{ for } \sigma_h^2(n) \to 0 \\ 1, \text{ for } \sigma_h^2(n) \to \infty \\ 0, \text{ for } \gamma_b \gg 1 \\ \gamma_b \frac{N_f \lg_2 L}{N_t} \sigma_h^2(n), \text{ for } \gamma_b \ll 1 \end{cases}. \quad (15)$$

These values correspond to those employed by receivers implemented according to the Maximal Ratio Combining (MRC) criterion [19] and, when $n = 0$ (flat-fading assumption), then (14.1) and (14.2) reduce themselves to decision statistics defined in [15,20] in the case of No Channel State Information (NCSI) at the receive side. When ($\mathcal{N}K$) and ($Lg\mathcal{N}$) fading are considered, then z_l in (13) is defined as follows:

$$z_l \triangleq \sum_{n=0}^{V+1} \sum_{j=1}^{N_r} \sum_{i=1}^{N_t} \ln \left\{ \cosh \left[\varphi_n (\underline{\mathbf{y}}_j(n)^T \underline{\mathbf{e}}_i(l)) \right] \right\} \quad (16.1)$$

where

$$\varphi_n = \begin{cases} 2\sqrt{2}\left[2\left(1+\frac{2mN_t}{\sigma_h^2(n)\lg_2 LN_f}\right)\right]^{-\frac{1}{2}}, (\mathcal{N}K \text{ fading}) & (16.2) \\ \sqrt{\frac{\lg_2 L\gamma_b N_f}{N_t}}e^{c\mu_n}, \qquad (Lg\mathcal{N} \text{ fading}) & (16.3) \end{cases}$$

being $\mu_n(dB) \triangleq \mathrm{E}\{\alpha_n(j,i)\} = \frac{1}{2c}\ln\left(\sigma_h^2(n)\right) - c\sigma_r^2$, where $c = 1/20\ln 10 = 0.115$.

A. Union-Chernoff bounds on the Symbol Error Probability

Since the computation of the Symbol Error Probability (SEP) $P_E \triangleq P\left(\mathbf{\Phi} \neq \hat{\mathbf{\Phi}}_{ML}\right)$ of the ML decoder in (13) resists to closed-form analytical evaluations even in the limit case of flat-fading channels [5, 6, 11, 12, 13], in the sequel we resort to the Union-Chernoff approach to upper bound P_E. We anticipate that the resulting bounds have been derived for Unitary OPPM based STBCs with *Orthogonal* matrix codewords as in

$$\mathbf{\Phi}_m^T\mathbf{\Phi}_l = \mathbf{0}_{N_t}, \quad m \neq l. \tag{17}$$

In fact, by adopting Unitary and Orthogonal STBCs, the overall MIMO IR-UWB transceiver is able to work at the maximum of diversity gain attainable in *multipath* faded and *MIMO* scenario, as denoted by the expressions of Union-Chernoff bounds. Specifically, when $\mathcal{G}$ multipath fading is considered, then the resulting Union-Chernoff bound is given by the following expression:

$$P_E \leq (L-1)\prod_{n=0}^{V}\left[\frac{\left(1+\sigma_h^2(n)\frac{N_f}{N_t}(\lg_2 L)\gamma_b\right)}{\left(1+\frac{1}{2}\sigma_h^2(n)\frac{N_f}{N_t}(\lg_2 L)\gamma_b\right)^2}\right]^{\frac{N_tN_r}{2}}. \tag{18}$$

We remark that this limit generalizes the case of flat-fading and it is attained by setting $V = 0$ and $\sigma_h(0) = 1$ in (18). Second, when $(\mathcal{N}K)$ multipath fading is considered, the resulting Union-Chernoff bound expression can be expressed as

$$P_E \leq (L-1)\left(\frac{e^2\Gamma(2m)}{\Gamma(m)}\right)^{(N_rN_t(V+1))} \cdot \prod_{n=0}^{V}\left[\frac{mN_t}{4(\lg_2 L)N_r\sigma_h^2(n)\gamma_b}\right]^{mN_tN_r}, \tag{19}$$

where $\Gamma(.)$ denotes the Gamma Function and m stands for the Nakagami factor. Lastly, the Union-Chernoff bound for $(Lg\mathcal{N})$ path gains has been also derived, but it cannot be expressed in closed form, because it is composed by the sum of pairwise error probabilities $\left\{P_{lm} \triangleq P\left\{\hat{\mathbf{\Phi}}_{ML} = \mathbf{\Phi_m} \mid \mathbf{\Phi} = \mathbf{\Phi_l}\right\},\ l \neq m\right\}$ assuming the following expression

$$P_{lm} \leq \prod_{n=0}^{V}\prod_{j=1}^{N_r}\prod_{i=1}^{N_t}\left\{e^{\left(\frac{1}{2}e^{c\mu_n}\varphi_n C_1\right)} \left\{\mathrm{E}\left\{sech\left(C_1\varphi_n e^{r_n(i,j)}\right)\right\}\right\}\right\}, \tag{20}$$

where the function $sech(.)$ denotes the hyperbolic secant and the expectation in (20) is upper limited as in

$$\mathrm{E}\left\{sech\left(C_1\varphi_n e^{r_n(i,j)}\right)\right\} \leq 2\mathrm{E}\left\{\exp\left(-C_1\varphi_n e^{r_n(j,i)}\right)\right\} = \frac{2}{\sqrt{\pi}}\int_{-\infty}^{\infty}\exp\left(-t^2 - C_1\varphi_n e^{c\sqrt{2}\sigma_r^2 t}\right)dt. \tag{21}$$

Now, in order to evaluate the diversity gain achieved by the proposed transceiver for the above three cases, let us start to consider the Union-Chernoff bounds closed forms (18) and (19). We have ascertained that both limits result to be tight and asymptotically exact at medium/high SNR γ_b (e.g., they vanish for increasing γ_b), and furthermore, they are constituted by a number of product terms equal to the number of the arrivals (e.g., $(V+1)$), while the exponent terms are $N_rN_t/2$ and mN_rN_r for the $(\mathcal{G})$ and $(\mathcal{N}K)$ fading, respectively. This allows us to conclude that at medium/high SNR γ_b the corresponding system SEPs is able to fall (at the most) as $O(\gamma_b^{-N_tN_r(V+1)/2})$ and $O(\gamma_b^{-mN_tN_r(V+1)})$ for these two cases. Such results *confirm* what anticipated at the beginning of this Sect.IV-A, that is the Orthogonal and Unitary STBCs are *optimal* in the sense that *all* the $(V+1)$ arrivals contribute to the final system diversity gain. If we compare this result with those found in [5, 11, 13], which are valid for MIMO *carrier-modulated* system operating in $(\mathcal{G})$ flat-fading condition, it appears to be in $sharp\ contrast$ with them, because they show a diversity gain equal to N_tN_r. Actually, this difference can be justified by observing that IR-UWB systems are *baseband* so that the corresponding channel path gains $h_n(j,i)$ are *real-valued*.

V. The proposed STOPPM codes

The Space Time Orthogonal Pulse Position Modulated (STOPPM) codes we propose constitute a class of variable-rate unitary OPPM-based STBCs, characterized by the following two definitory properties:

i) the size M of the employed OPPM modulation equates the product LN_t, that is,

$$M = LN_t; \tag{22}$$

ii) the N_t columns of the l-th $(M \times N_t)$ matrix codeword $\mathbf{\Phi}_l$, $0 \leq l \leq L-1$, are constituted by the N_t unit-vectors of $\mathbb{R}^M$ with index i ranging from $i = lN_t$ to $i = (l+1)N_t - 1$, that is,

$$\mathbf{\Phi}_l \triangleq [\underline{\mathbf{e}}(lN_t)\ ...\ \underline{\mathbf{e}}((l+1)N_t - 1)],\ \ 0 \leq l \leq L-1. \tag{23}$$

The so-defined STOPPM codes retain some interesting key-properties we detail in the sequel. First, since the N_t columns of each codeword are mutually-orthogonal unit-vectors (see (31)), we have that

$$\mathbf{\Phi}_l\mathbf{\Phi}_l^T = \mathbf{I}_{N_t}, \quad 0 \leq l \leq L-1. \tag{24}$$

so that the STOPPM are *unitary* STBCs.

Second, since the $2N_t$ columns of any pair of distinct codewords $\mathbf{\Phi}_l$ and $\mathbf{\Phi}_m$ (with $l \neq m$) are mutually orthogonal vectors, according to (17).

Third, after considering the expression of T_p reported in (5), the spectral efficiency of a STOPPM code is

$$\eta_B = \frac{(-\lg_2 Lln(1-\eta))}{L\lambda N_f \left(T_\mu - \frac{ln(1-10^{-2})}{\lambda}\right)}, \quad \text{(bit/sec/Hz)}. \qquad (25)$$

Finally, from the unitary and orthogonality properties in (4), (5), it arises that the Bit-Error-Probability $P_E^{(b)}$ of a STOPPM code is related to the corresponding SEP P_E via the following (simple) relationship

$$P_E^{(b)} = [L/(2(L-1))]P_E. \qquad (26)$$

VI. Simulation Setup and Numerical Results

To test the actual performance of the presented MIMO IR-UWB transceiver of Figs.1,2, equipped with the proposed STOPPM codes of Sect.V, we have carried out several numerical trials. The (unit-energy) monocycle $p(t)$ used by all the tested systems to convey the information data is the second time-derivative of the Gaussian pulse (e.g.,[1], [18, Sect.1.3]).

A. Diversity and Coding Gains of the STOPPM codes over spatially uncorrelated channels and multipath effects

All the performance plots reported in Figs.1, 2 refer to IR-UWB systems with spectral efficiency $\eta_b \approx 1/5000$(bit/sec/Hz) operating over spatially uncorrelated faded CM2 channel. An examination of these plots leads to two main conclusions. First, as shown by Fig.1, the proposed transceiver equipped with the STOPPM codes achieves the best performance in a Multipath $Lg\mathcal{N}$ fading environment with a slope equal to $2N_tN_r(V+1)$, while the intermediate performance are attained for $\mathcal{N}K$ fading with typical values of Nakagami factor, (e.g., $m = 0.8$, $m = 1.4$) and slopes on the order of $mN_tN_r(V+1)$.

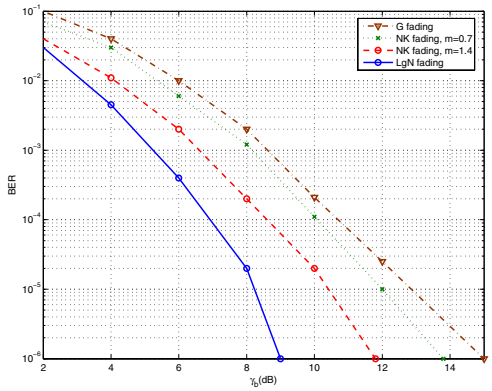

Fig. 1. Simulated performance of MIMO IR-UWB systems equipped with STOPPM codes. Case of $L = 2$, $N_r = 1$, $N_t = 3$ $\eta_B = 1/5000$(bit/sec/Hz) and CM2 channel.

The worst case results to be the $\mathcal{G}$ fading with slope on the order of $N_tN_r/2$. Specifically, in terms of SNR gain, this MIMO transceiver presents a SNR gain of 2.8dB passing from $\mathcal{N}K$ with $m = 1.2$ to $Lg\mathcal{N}$ fading and 1dB from $\mathcal{N}K$ with $m = 0.8$ to $\mathcal{G}$. Second, as shown by Fig.2, when the transceiver works in a $Lg\mathcal{N}$ fading environment the gain approaches 1, 1.5, and 2 order of magnitude with respect to the case of the SISO version, when the number of transmit antennas is limited to $N_t = 2$, $N_t = 3$ and $N_t = 4$, respectively. Moreover, these BER gaps fast increase, thus confirming the optimality of the STOPPM codes both in terms of diversity and coding gains.

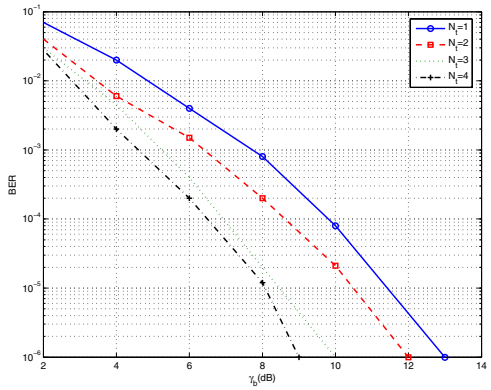

Fig. 2. Simulated performance of MIMO IR-UWB systems equipped with STOPPM codes. Case of $L = 2$, $N_r = 2$, $\eta_B = 1/5000$(bit/sec/Hz) and CM2 channel and $Lg\mathcal{N}$ distributed multipath fading.

B. Coverage Range Extension allowed by STOPPM Codes

The BER improvement resulting by the adoption of the STOPPM codes may be turned into a corresponding coverage range extension, when the considered IR-UWB systems are forced to operate at an assigned (e.g., fixed target BER). Thus, to test the range-extension capabilities actually offered by the MIMO transceiver of Figs. 1, 2 over the corresponding SISO's one, we have implemented IR-UWB links affected by path-loss modelled in [3] and typically valid for $(\mathcal{G})$ distributed path gains (outdoor applications). The corresponding coverage ranges are summarized in Table 1. An examination of numerical results reported in this Table leads to the following conclusions. First, the considered operating conditions, by passing from $N_t = N_r = 1$, (e.g., SISO systems) to $N_t = N_r = 2$ the coverage ranges increase by a factor approximately equal to 4.5 when CM2 is adopted. Moreover, these increasing factors approach about 1.32 when we pass from $N_t = N_r = 2$ to $N_t = 2$ and $N_r = 3$. Second, the MIMO IR-UWB systems with $N_t = N_r = 2$ and STOPPM codes attain coverage range exceeding 130mt, thus allowing the utilization of these systems for *outdoor medium-range* applications.

C. Spatial Correlation

When the spatial correlation of the channel coefficients within the MIMO UWB-IR is considered (the adopted antennas are not sufficiently spaced apart and/or we consider low-scattered environments as underlined in [3,14]), then we need to model the MIMO UWB-IR channel model to consider

N_t	N_r	Coverage Ranges (in mt.)
1	1	30
2	1	68
3	1	87
2	2	137
2	3	181

TABLE I

COVERAGE RANGES OF MIMO IR-UWB SYSTEMS USING STOPPM CODES. $A_b = A_{sys} = 1$, BER IS 10^{-6}, POWER IS 2.5 MW, AND THE CHANNEL MODEL IS CM2.

this effect and to specify the spatial covariance matrices $\mathbf{R}_n^{T_x}$ and $\mathbf{R}_n^{R_x}$. In this regard, we have considered a MIMO system equipped with $N_t = N_r = 2$ antennas and equicorrelated path gains. Specifically, the resulting covariance matrices can be write as

$$\mathbf{R}_n^{R_x} = \begin{pmatrix} 1 & c_r \\ c_r & 1 \end{pmatrix}$$
$$\mathbf{R}_n^{T_x} = \begin{pmatrix} 1 & c_t \\ c_t & 1 \end{pmatrix} \tag{27}$$

where the terms $\{c_r, c_t \in [-1, 1]\}$ denoting the correlation coefficients at the receive and transmit side respectively, that is

$$c_r \triangleq \frac{\mathrm{E}\{h_n(j,i)h_n(f,i)\}}{\sqrt{\mathrm{E}\{h_n^2(j,i)\}}\sqrt{\mathrm{E}\{h_n^2(f,i)\}}}, \tag{28}$$
$$1 \le i \le 2, \;\; 1 \le j, f \le 2, \;\; j \ne f,$$
$$c_t \triangleq \frac{\mathrm{E}\{h_n(j,i)h_n(j,q)\}}{\sqrt{\mathrm{E}\{h_n^2(j,i)\}}\sqrt{\mathrm{E}\{h_n^2(j,q)\}}}, \tag{29}$$
$$1 \le i, q \le 2, \; 1 \le j \le 2, \;\; i \ne q.$$

The spatial correlation effect reduces the system diversity order, as experienced also by a worsening in terms of BER of the proposed MIMO UWB-IR transceiver. By observing Fig.3, it results as an evidence that the system robustness is held for spatial correlation values up to $\mid 0.6 \mid$. This correlation term carries to SNR losses within 2dB. Furthermore, this result agrees with the channel measurement campaigns where the spatial correlation is typically low and it is usually negligible (not taken into account) for the optimization of UWB transceivers [3,7].

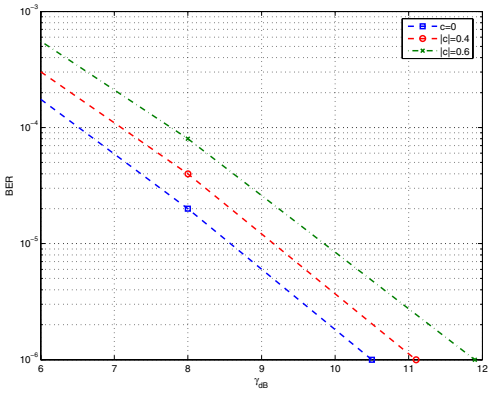

Fig. 3. System robustness when the channel coefficient are spatially correlated, when the Log-Normal Multipath Fading is considered and the channel model is CM1. The number of antennas is $N_t = N_r = 2$, while the number of frames is $N_f = 4$.

REFERENCES

[1] M.Z.Win, R.A.Sholtz, "Ultra Wide Bandwidth Time-Hopping Spread-Spectrum Impulse Radio for Wireless Multiple-Access Communications", IEEE Trans. on Comm, vol.48, pp. 679-691, Apr. 2000.

[2] L.Yang, G.B.Giannakis, "Space-time Coding for Impulse Radio", IEEE Conf. on Ultra Wide Band Syst., pp. 235-239, 2002.

[3] K.Siwiak, A.Petroff, "A Path Link Model for Ultra Wide Band Transmission", IEEE VTC2001, Rhodes, Greek, May 2001.

[4] L.Yang, G.B.Giannakis, "Analog Space-Time coding for Multi-Antenna Ultra Wide Band Transmissions", IEEE Trans. on Comm., vol. 52, pp. 507-517, Mar. 2004.

[5] J.C.Guey, M.P.Fitz, M.R.Bell, W.Y.Kuo, "Signal Design for transmitter diversity wireless communication systems over Rayleigh fading channels", IEEE Trans. on Comm., vol. 47, pp. 527-537, Apr. 1999.

[6] X.Zhu, R.D.Murch, "Performance Analysis of Maximum Likelihood Detection in a MIMO antenna system", IEEE Trans. on Comm., Vol.50, pp. 187-171, Feb.2002.

[7] FCC, First Report and Order, FCC-02-48, "Revision of Part 15 of the Commission's rules regarding Ultra Widebnad transmission systems", adopted February 14, 2002.

[8] J.H.Reed, et Alii, An introduction to Ultra Wide Band Communication Systems, Ed. Prentice Hall, 2005.

[9] V.Pohl, V.Jungnickel, C.von Helmot, "The Algebraic Structure of Frequency-Selective MIMO channels", IEEE Trans. on Signal Processing, vol.53, no.7, pp. 2498-2592, July 2005.

[10] G. Yue, L.Ge and S.Li "Performance of UWB time-hopping spread spectrum impulse radio in multipath environment", Proc. IEEE Vehicular Technology, pp1644-1648, Seoul (Korea), Apr. 2003.

[11] A.Paulray, Introduction of Space-Time Wireless Commmunications, Cambridge Univ. Press, 2003.

[12] E.Baccarelli, M.Biagi, "Performance and Optimized Design of Space-Time Codes for MIMO Wireless Systems with Imperfect Channel-Estimates ", IEEE Trans. on Signal Processing, Vol.52, no.10, pp.2911-2923, Oct. 2004.

[13] B.M.Hochwald, T.L. Marzetta, "Unitary space-time modulation for multiple-antenna communications in Rayleigh flat fading", IEEE Transactions on Inform. Theory, Vol.46, no.2, pp. 543-564, March 2000.

[14] S.Roy, J.R.Foerster, V.S.Somayazulu, D.G.Leeper, "Ultrawideband radio design: the promise of high-speed, short-range wireless connectivity", Proceedings of the IEEE, Vol.92, no.2, pp. 295-311, Feb. 2004.

[15] E.Baccarelli, M.Biagi, C.Pelizzoni, P.Bellotti, "A Novel Multi-Antenna Impulse Radio UWB Transceiver for Broadband High-Throughput 4G WLANs", IEEE Comm. Letters, vol.8, no.7, pp.419-421, July 2004.

[16] E.Baccarelli, M.Biagi, R.Bruno, M.Conti, E.Gregori, Broadband Wireless Access Networks: a Roadmap on Emerging Trends and Standards, in Broadband Services: Business Model and Technologies for Community Networks, pp. 215-240, Wiley, 2005.

[17] K.Yu, B.Ottersen, "Models for MIMO propagation channels: a review", Wireless Comm. and Mob. Comp., vol.2, pp. 653-666, July 2002.

[18] J.Foester, P802.15-02/490rl-SG3a-Channel modelling Subcommittee-Report Final.doc , available on http://grouper.ieee.org/groups/802/15/pub/, Mar 2003.

[19] J.G. Proakis, Digital Communications, 4-th ed., Mc-Graw Hill, 2001.

[20] E.Baccarelli, M.Biagi, C.Pelizzoni, N.Cordeschi, F.Garzia, "Space-Time Orthogonal M-ary PPM (STOMP) Coding for Coverage Extension of UWB-IR Systems", Intern. Symp. of Wireless Comm. Syst. 2005 (ISWCS 2005), Siena, pp. 263-267, Sept 2005.

[21] H.Liu, R.C.Qiu, Z.Tian, "Error Performance of Pulse-Based Ultra-Wideband MIMO Systems Over Indoor Wireless Channels", IEEE Tr. on Wireless COmmunications, Vol.4, No.6, pp.2939-2944, Nov.2005.